ME555

FINAL PROJECT REPORT

DESIGN OPTIMIZATION OF A CLOSED-LOOP MEMS ACCELEROMETER

RAGHAV PAUL

25 April 2014

Abstract

This study aims to optimize the Full Scale Range and Minimum measurable acceleration of a MEMS accelerometer operating in Closed Loop mode. Certain geometrical constraints like packaging, engineering constraints like critical voltage and mechanical constraints like stiffness ratios constrain the objective from growing without bound. These are implemented in the SQP algorithm to comb through the design space and obtain the optimal point. A Pareto curve was generated that reflects the tradeoffs between optimizing both the objectives and parametric studies are carried out to understand the dependence of the optimal point on the value of these parameters. An optimal design is stated and analyzed for Lagrangian multipliers and bounds.

1. INTRODUCTION

1.1 MEMS is a relatively new field of study that started in the 1950s. However large scale manufacturing increased exponentially only in the 90s where applications like accelerometers, digital micro-mirrors, RF MEMS and Optical Imaging developed. At this point, the oldest (and declining) application for MEMS is Inkjet heads and filters and on the other end of the spectrum, MEMS speakers and micro-fuel cells are emerging.

Accelerometers, another MEMS application, are currently in the maturity phase of their cycle, with a total business of $1000m each year, most of which is contributed by smarthphones. However, it is believed that there is considerable room for improvement even in existing designs and optimization is one of the ways to move in that direction. This study aims to study how certain performance metrics can be improved simply by changing design variables involved in a single design.

Working within the design space, we need to impose certain engineering constraints which pertain to the geometric, mechanical and electrical properties of the device.

By employing well-known optimization algorithms that efficiently comb through the design space, it is possible to identify certain combinations that maximize the given objectives. Further, parametric studies are performed to study the variation in the optimized performance. Finally, to balance different requirements, some choices need to be made regarding which objective would be given higher preference. This is presented in terms of a Pareto graph that reflects these tradeoffs.

1.2 MEMS Accelerometers working procedure

Accelerometers work on the principle of pseudo-forces generated on masses in response to external motion. A free-body diagram of an accelerometer is given in Figure 1.

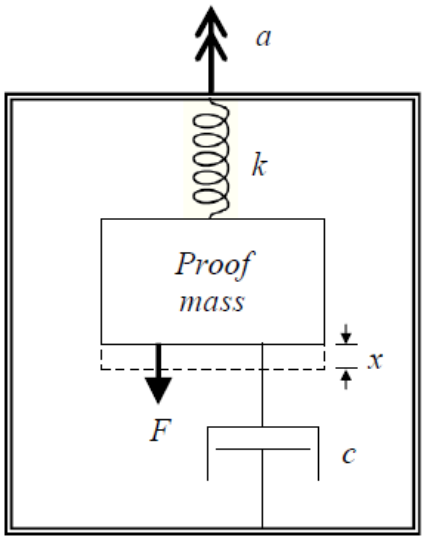

Figure 1. FBD of an accelerometer

In response to external acceleration, the proof mass, suspended by a spring and a damper, will move a certain distance x. By measuring this distance, we can calculate the original acceleration that the mass was subjected to. To embed electronics into the device, the change in capacitance between two plates is measured, one of which is connected to the proof mass.

Figure 2. shows a lumped-mass model of the accelerometer.

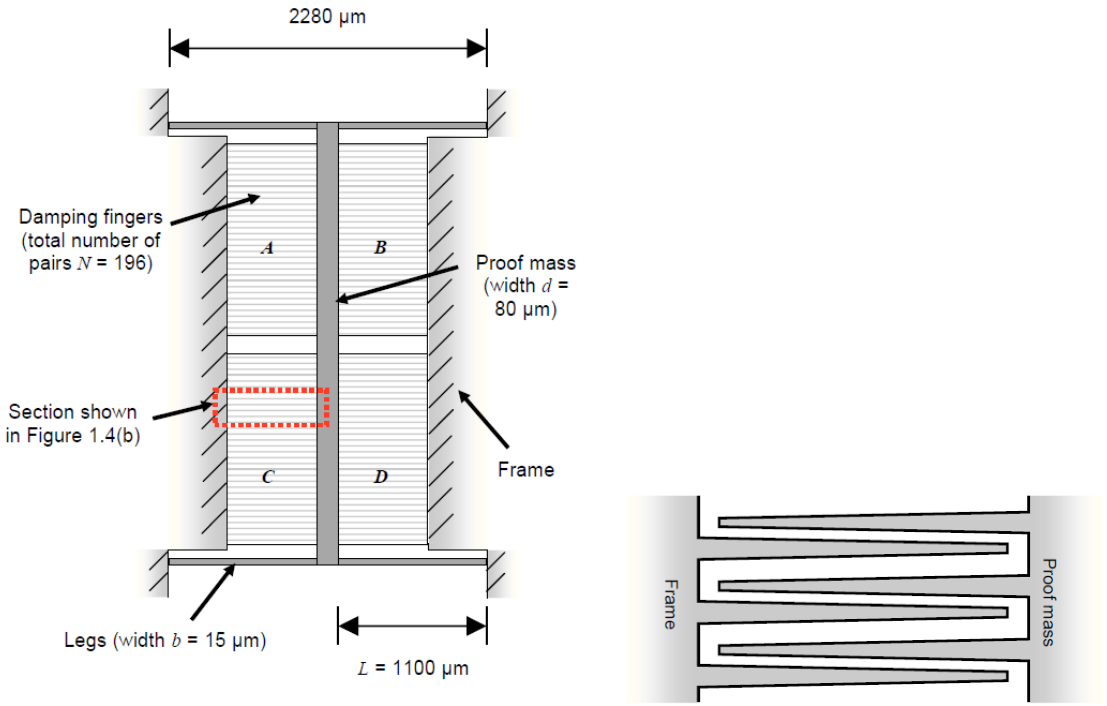

Figure 2.

The proof mass is suspended to a rigid frame by four rigid legs which provide the compliance to motion. N damping fingers are attached to the proof mass which move along with proof mass. The capacitance measurement system described above is implemented with this set of fingers along with a set of fingers attached to the frame.

1.3 Closed Loop Operation

Closed-loop operation of the accelerometer is superior to the conventional open-loop version described above. It eliminates the need for the proof mass to move and instead relies on measurements of feedback Voltage to determine external acceleration.

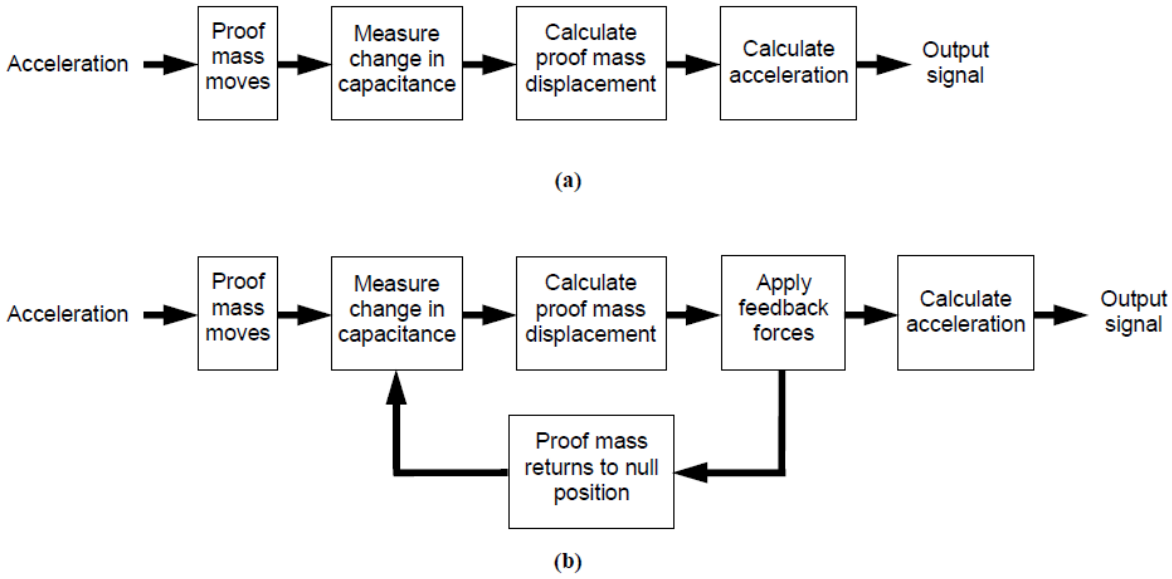

Figure 3.

Figure 3a and 3b shows the comparison between the two modes of operation. At the heart of the closed loop scheme is a feedback mechanism that senses when the proof mass is trying to move away from the closed-loop operation. Then the voltage across the 'capacitor' plates is changed by a sophisticated control system to maintain the neutral position. By measuring how much effort was required to keep the mass at the equilibrium point, we can back-calculate the external acceleration.

While open-loop operation eliminates the need to design complicated electronics, closed loop operation is more robust in that there are no moving parts in the device.

2. DESIGN PROBLEM

This study aims to optimize the Full Scale Range, defined as the difference between maximum and minimum measurable accelerations and the threshold minimum acceleration. Both these performance metrics are important figures of merit for any accelerometer design. Some other metrics like Bandwidth (related to response time), bias, sensitivity, maximum feedback voltage are ignored to keep the model simple and tractable.

Certain parameters like the first natural frequency and damping ratio are kept within certain bounds to satisfy engineering criteria as described in the Constraints section.

The fabrication of MEMS accelerometers is another related field of study. Basically it involves etching of a starting wafer with the help of masks that transfer the pattern onto the substrate. DRIE, or deep Reactive Ion Etching is the most commonly used process in other MEMS manufacturing processes as well. The only limitation that manufacturing can have on the optimization process is the maximum aspect ratio that can be produced by DRIE. If the algorithm requires excessively thin and long sections, it may not be possible to fabricate them by traditional processes.

2.1 MODELING

As described in the introduction, closed loop operation always brings the device to the equilibrium point. To model the feedback forces, consider the following development.

2.1.1 Feedback forces

In the actual system, the restoring force is applied via a change in the Duty Cycle rather than changing the actual voltage at each point.

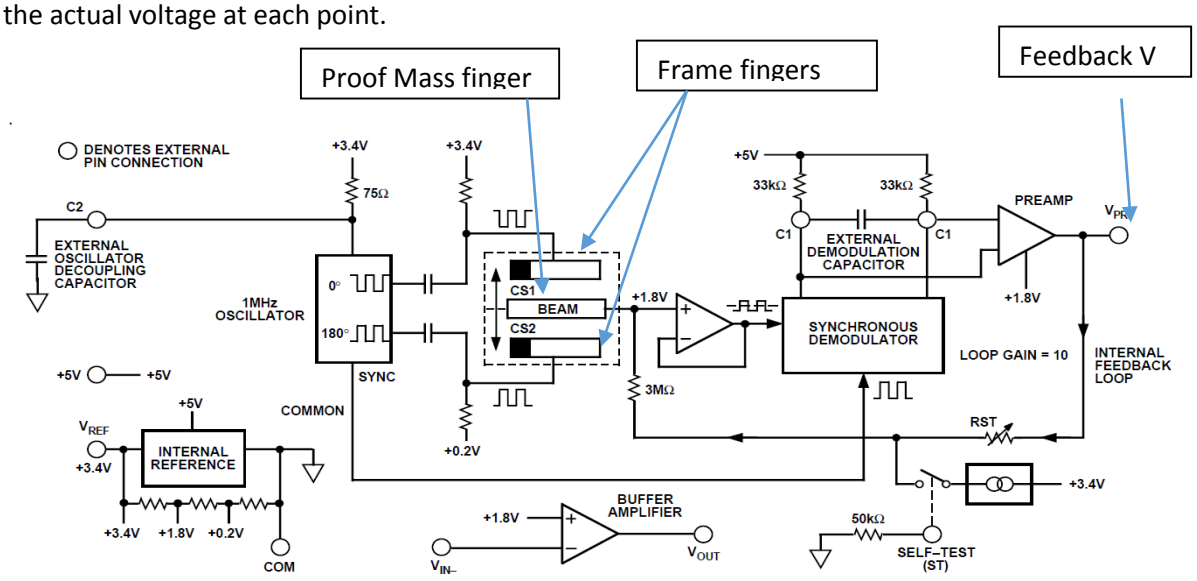

Figure 5.

The circuit from Figure 5. Is from one of the commercially available accelerometers, the ADXL 50. Without external acceleration, the Frame fingers apply a square wave of around 1MHz to the proof mass. This is such a fast frequency that the proof mass effectively remains at rest. When acted upon an external acceleration, The feedback voltage V changes to bring the proof mass back. The synchronous demodulator compares the voltage in the rest phase and the current voltage in the displaced phase to provide a negative feedback voltage.

The force between two capacitor plates is given as

$$F = \frac{N\varepsilon h l_f V_0^2}{2t^2}$$

Accounting for the changes the duty cycle, the formula for the feedback force (F_{fb}) becomes

$$F_{fb} = \frac{N\varepsilon h l_f V_0^2}{2}\left[\frac{D}{t^2} - \frac{1-D}{t^2}\right]$$

The full scale range is nothing but the maximum acceleration measurable by the device. That is nothing but the maximum value of the feedback force (assumed to be at a Duty Cycle of 0.9 is)

$$FSR = \frac{F_{\max}(\mathrm{D} = 0.9)}{m}$$

This concludes the derivation of one Objective function. The other one is the threshold minimum acceleration measurable by the device.

2.1.2 Threshold acceleration

The capacitance between 2 plates is given as

$$C\ (x) = \frac{\varepsilon A}{t \pm x}$$

Where the ε is the permittivity of the space, t is the nominal distance before the displacement x. Differentiating this w.r.t x,

$$\frac{dC}{dx} = \frac{\pm \varepsilon A}{(t \pm x)^2}$$

This suggests that the minimum distance the proof mass would move had there been no feedback mechanism is

$$a_{\min} = \frac{kt}{mC_0} \Delta C_{\min}$$

As can be seen from the equation above, the value of amin is dependent on the minimum measurable capacitance. This is dependent on the electronics and the associated noise floor. For this study, a noise floor of 4e-18 was used as the value for $\Delta C_{\min}$.

2.1.3 Squeeze Film Modeling

The casing of the accelerometer is filled with an inert gas, in this case Nitrogen was used. Flow between the two plates was modeled as Coutte flow with the damping factor and damping coefficient given as

$$\gamma = b\sqrt{km};$$
$$b = \frac{96\eta l_f h^3 N}{\pi^4 t^3}$$

2.1.4 Natural Frequencies of vibration

Natural frequencies of vibration are extremely important in the formulation of the design problem. For the proof mass the modes that are usually present are 1. In-plane mode 2. Out-of-plane 3. Sideways in plane. These are shown in Figure 6.

These modes were calculated on the basis of Rayleigh's method. This method effectively equates the maximum kinetic and potential energy. For the in-plane mode, which is the most important of the modes, the formulation is as follows:

$$\omega_1 = \frac{1}{2\pi}\sqrt{\frac{3NEI_y}{\frac{13}{140}\rho w_s hNl_s + \frac{1}{4}ml_s^3}}$$

The value for the second natural frequency is given in the MATLAB code and utilizes the Rayleigh's method as well.

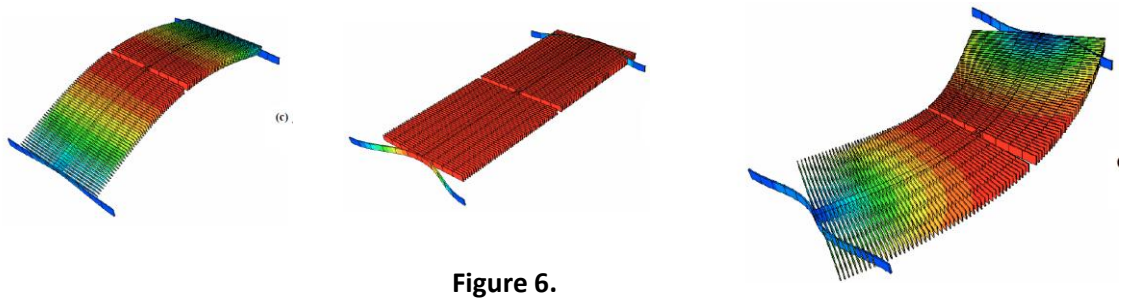

Figure 6.

2.1.5 Critical Voltage

The critical voltage is another important consideration in the design of the accelerometer. The device may get 'stuck' if the feedback forces are not able to bring the mass to the equilibrium position. This situation occurs when there is a 'negative' spring constant associated with the proof mass. This is a very common problem associated with all MEMS devices that use Voltage for actuation. To determine the Critical voltage, we need to equate the derivative of the electrical force and the mechanical spring constant. In other words,

$$\frac{dF_{fb}}{dx} = k$$

This relation leads to the critical voltage being:

$$V_{critical} = \sqrt{\frac{kt^3}{2\varepsilon l_f hN}}$$

The constraints associated with the optimization problem are explained after the summary.

SUMMARY OF DESIGN PROBLEM

The objectives to be optimized in this study were the full scale range and the threshold minimum acceleration to be measured by the MEMS accelerometer.

S.No.	Objective	Physical Interpretation
1	FSR	Full Scale Range
2	a_min	Threshold minimum acceleration

Table 1

Some engineering constants and parameters were used in the study, they are given below;

S.No	Variable	Physical Interpretation	Value
1	h	Wafer thickness	135 μm
2	E	Young's Modulus of <100> Silicon	1.3e11 Pa
3	η	Viscosity of Nitrogen gas	1.6629e-5 Pa.s
4	ρ	Density of <100> Silicon	2330 kg/m^3
5	ε	Permittivity of Nitrogen (air)	8.85418782 × 10-12 m^{-3} kg^{-1} s^4 A^2
6	ΔC	Minimum measurable capacitance	100 μF

Table 2

A list of variables in the optimization process is given below:

S.No.	Variable	Physical Interpretation
1	L_s	Length of leg
2	W_s	Width of leg
3	L_p	Width of proof mass
4	W_p	Length of proof mass
5	N	Number of damping fingers
6	L_f	Length of damping finger
7	W_f	Width of damping finger
8	t	Initial gap between fingers
9	V_0	Square wave voltage

Table 3

.

The following constraints were used in the optimization;

S.no	Constraint Type	Physical Meaning	Linear/Non-linear	Definition
1	Geometrical	Packaging constraint – horizontal dimension should not exceed 5mm	Linear	2*Ls+W_p<5e-3
2	Geometrical	Packaging constraint – vertical dimension should not exceed 5mm	Linear	2*W_s+L_p<5e-3
3	Geometrical	Length of damping fingers should be smaller than length of Length of legs	Linear	L_f<L_s
4	Geometrical	Total number of fingers should fit on proof mass	Non –linear	N*(2*t+W_f+1e-6)-L_p<0
5	Mechanical	Ratio of stiffness out-of-plane bending to in-plane bending should be more than 10	Non-linear	$\frac{K_z}{K_x} - 10 > 0$
6	Mechanical	Ratio of stiffness transverse-plane bending to in-plane bending should be more than 5	Non-linear	$\frac{K_y}{K_x} - 10 > 0$
7	Mechanical	Damping ratio should be close to .0707 (Within a tolerance of ε)	Non-linear	$\gamma - 0.707 < \varepsilon$
8	Mechanical	First mode of vibration should be greater than 1 KHz	Non-linear	ω_1 >1Khz
9	Mechanical	First two modes must be separated by atleast 10 KHz	Non-linear	$\omega_2 - \omega_1 > 10KHz$
10	Electrical	Critical Voltage must not be exceeded	Non-linear	V<$V_{critical}$

Table 4

Geometrical Constraints:

The geometrical constraints 1, 2, 3 and 4 given in the table are self-explanatory and are necessary for the physical realization of the device.

Mechanical Constraints

Constraint 5 and 6

These constraints have to be enforced to ensure that the proof mass maintains its rigidity in all directions other than the sense direction. Therefore, out-of-plane and transverse-direction stiffness is kept 10 and 5 time larger than the in-plane stiffness. Details of the derivation can be found in the Progress Report.

Constraint 7

The damping ratio of the device should be close to 0.707 as this value balances for overshoot and settling time. Any deviation from this value either increases overshoot or settling time. A window of 0.1 was kept in the optimization.

Constraint 8

In practice, MEMS accelerometers are subject to a variety of environments were external vibrations are aplenty. Keeping the first mode of vibration greater than 1 KHz partly ensures that the device will not be excited by stray external vibrations.

Constraint 9

The first two modes of vibrations should be kept apart by atleast 10 Khz to ensure that there is no inter-modal coupling in the device.

Electrical Constraints

Critical Voltage causes instability in the MEMS device and does not permit the feedback forces to attract the proof mass back to its equilibrium direction. If this constraint is not enforced, the operating voltage may exceed the Critical voltage at times requiring the device to be reset periodically.

Model Bounds

Based on common engineering assumptions, some bounds were fixed on the variables for the results of the optimization to make sense. These are detailed in the following table

Variable	**Minimum value**	**Maximum value**
L_s	100 **μ**m	4000 **μ**m
W_s	2 **μ**m	75 **μ**m
L_p	5 **μ**m	5000 **μ**m
w_p	200 **μ**m	1500 **μ**m
N	10	600
L_f	100 **μ**m	4000 **μ**m
W_f	3 **μ**m	30 **μ**m
t	1 **μ**m	3 **μ**m
V0	0.1 V	5V

Table 5

Some of the geometrical bounds follow from engineering thumb-rules while others are taken from literature, notably the thesis by Coultate. The voltage, for instance, is kept below 5 V as that is typically the highest voltage that commercially available electronics can power the accelerometer.

Optimization Results

There is no monotonic behavior in the model as all functions are non-linear contain a mass term, which is itself a non-linear function of the variables.

The MATLAB function fmincon was used in the optimization process. SQP was used as the solver and all other default options were used. The initial point was taken to be an existing design – the BAE 70 accelerometer. This strategy uncovered multiple minima in both the objectives. Results for independently optimizing the FSR and threshold acceleration are given below:

S.No.	Variable	Physical Interpretation	Optimized value for FSR
1	L_s	Length of leg	133.92 um
2	W_s	Width of leg	16.62 um
3	L_p	Width of proof mass	200 um
4	W_p	Length of proof mass	60 um
5	N	Number of damping fingers	10
6	L_f	Length of damping finger	133.92 um
7	W_f	Width of damping finger	3 um
8	t	Initial gap between fingers	1 um
9	V_0	Square wave voltage	5 V
	FSR	**Full Scale Range**	**6.35e2 g**

Table 6

S.No.	Variable	Physical Interpretation	Optimized value for amin
1	L_s	Length of leg	1300 um
2	W_s	Width of leg	10.157 um
3	L_p	Width of proof mass	1500 um
4	W_p	Length of proof mass	4600 um
5	N	Number of damping fingers	10
6	L_f	Length of damping finger	1300um
7	W_f	Width of damping finger	30 um
8	t	Initial gap between fingers	2.79 um
9	V_0	Square wave voltage	5 V
	A_min	**Threshold Minimum Acceleration**	**8.19e-3 g**

Table 7

Due to the multiple minima around different initial points, the Multi-start solver was used with 200 intial conditions close to the previous initial condition. This gave the same result even if Multi-start was used even with more initial points. Since the problem is not convex, there is no way of knowing whether this is the global optimal point, but under reasonable engineering judgment, it is.

A Pareto curve was formed that presents the tradeoff between the two objective functions. Depending on the commercial application, minimizing one of the two objectives may be more important than the other. The Pareto curve shown in Figure 7. Defines the relationship between the optimal values of each of the objective functions.

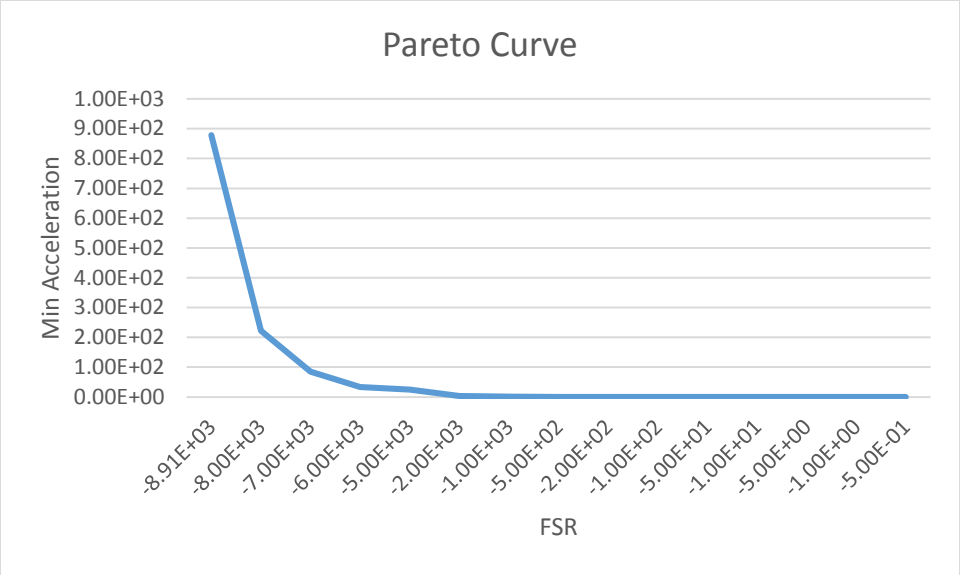

Figure 7

ANALYSIS OF THE RESULTS

Some values for the variables are right at either the upper or lower bounds provided in the model.

For example, the number of damping fingers stuck to its lower bound of 10 (Lagrange multiplier (L.M.) of 5.77e-5),while the the width of the damping fingers (LM=), the voltage and the width of the proof mass (LM =0.2892)reached their upper bound.

The values of multipliers corresponding to the different constraints are given in Table 8:

S.no	**Physical Meaning**	**Linear/Non-linear**	**Lagrange Multiplier**
1	Packaging constraint – horizontal dimension should not exceed 5mm	Linear	0
2	Packaging constraint – vertical dimension should not exceed 5mm	Linear	0.0942
3	Length of damping fingers should be smaller than length of Length of legs	Linear	0.2307
4	Total number of fingers should fit on proof mass	Non –linear	0
5	Ratio of stiffness out-of-plane bending to in-plane bending should be more than 10	Non-linear	8.05e-6
6	Ratio of stiffness transverse-plane bending to in-plane bending should be more than 5	Non-linear	0
7	Damping ratio should be close to .0707 (Within a tolerance of ε)	Non-linear	6.9079e-4

8	First mode of vibration should be greater than 1 KHz	Non-linear	1.28e-6
9	First two modes must be separated by atleast 10 KHz	Non-linear	0
10	Critical Voltage must not be exceeded	Non-linear	0

Table 8

This shows that the problem is more sensitive to the geometrical constraints more than the electrical and mechanical constraints. This makes sense too, as there is no direct benefit of relaxing them unless a critical point is reached. For instance, the Voltage can be increased as much as possible if it is improving the objective as long as it is below the critical value.

Further conclusions are difficult to draw as there are multiple non-linear constraints each affected by almost similar number of variables.

Parametric Study

In the initial optimization problem, some constants were used – such as the wafer thickness, the material etc. A parametric study was conducted varying these parameters to identify the variation in the optimal value as these parameters are moved around. Figures 8 and 9 show the results.

An interesting feature of the parametric study relating to the material is that even if we use a different Silicon configuration – <111> instead of <100>, the change in the value of the optimal solution is drastic.

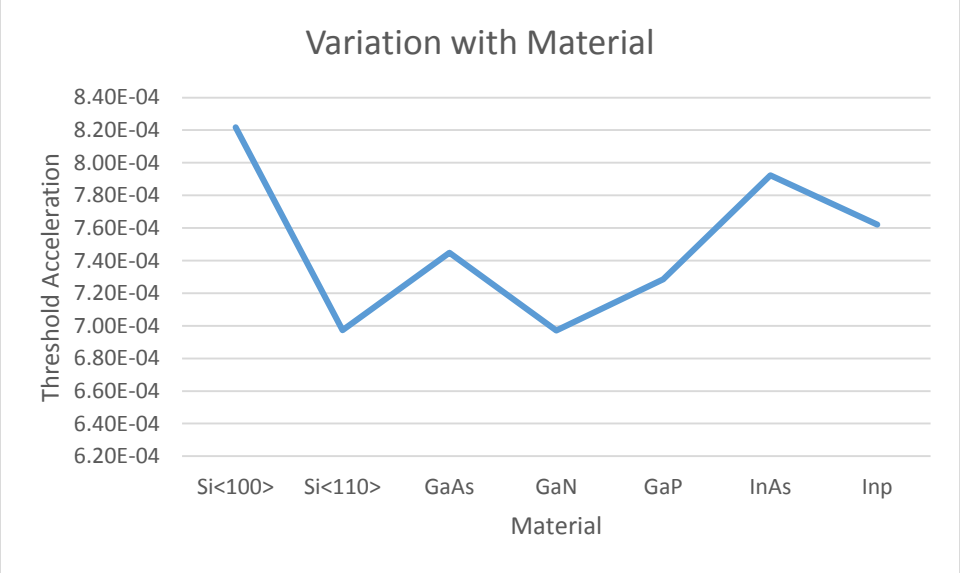

Figure 8.

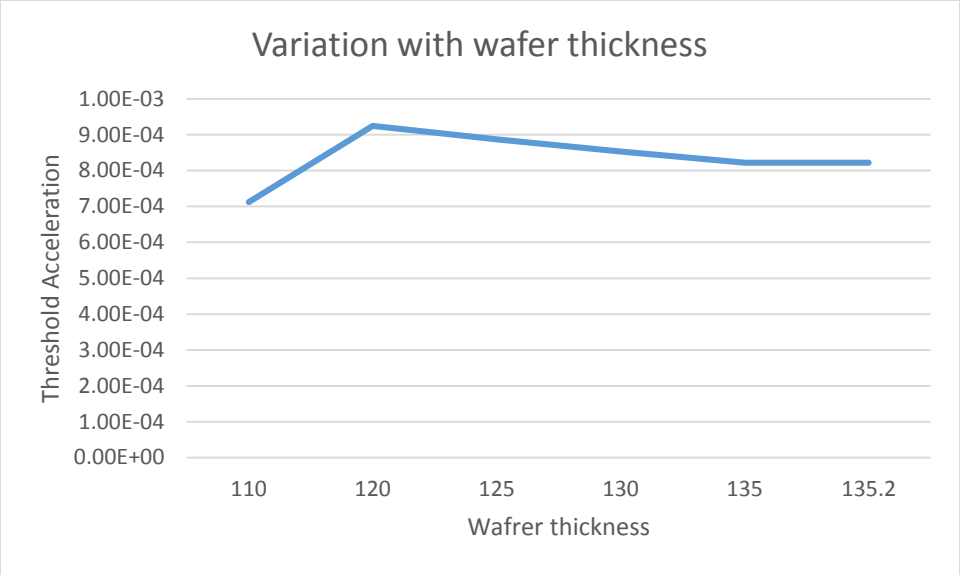

Figure 9

4. Discussion

The results make sense as these values correspond to the same range of values that commercially available accelerometers produce. The full scale range, is, however, on the higher side. This may be due to some factors that were left unaccounted for in the modeling phase. Some of them are listed below:

1. **Scaling**
   MATLAB handles a very high range in the variables effectively in this model. However, a more complex model may not be conducive to this range of values. Hence, scaling of the variables may be important.

2. **Interchangeability of modes**
   As the optimization algorithm combs through the design space, for some design dimensions, it may be possible that the second and third mode may get interchanged. This requires calculation of the third mode of frequency and implementing an if-else block in the code.
3. **Robustness**
   MEMS devices are very sensitive to changes in the characteristic dimensions. Further, as discussed in the introduction, the fabrication processes in MEMS are not advanced enough to provide the tight tolerances that are usually possible in macro-level processes. Taking the above into account, the algorithm should not pick out minima which are sharp valleys as it is likely that the design may end up varying slightly from the optimal point. Robustness is a different field altogether and integrating it with the current algorithm may be cumbersome.
4. **Tapering Fingers**
   The fingers fabricated in MEMS processes are usually tapering to facilitate removal after etching. This model assumed straight fingers, however it is not too tough to integrate this with the current model with the addition of more design variables.
5. **Bump stop**

A bump stop is usually included to prevent the proof mass moving too far in case a very high value of acceleration is applied. This could be integrated in the current algorithm with another design variable as the distance between the bump stop and the proof mass.

6. **Temperature Variation**
   Accelerometers are mounted in a range of environments that exhibit a lot of temperature variation. Although design is usually application specific, it may be possible to design 'globally' by including some variation in temperature. This point ties closely with Robustness of the device
7. **Bandwidth , Bias , Bias Stability, Sensitivity**
   These parameters are important objective functions like the full-scale range and threshold acceleration. Accelerometers are usually designed in-house with multiple teams like Mechanical and Electrical working together to meet a given set of specifications. Since this project did not focus on the electronics of the project, these objectives were neglected for optimization. However it may be possible to integrate this with the model by including variables that represent the parameters of the electronics.
8. **Etching rules**
   Etching rules state that the aspect ratio of the fabricated device may not exceed a particular value. This may be integrated easily with the current model.
9. **Finger yield Stress**
   The fingers acts as cantilever beams suspended from the proof mass. Although not a very important if the fingers are too long, this constraint may be developed easily.
10. **Open Loop Operation**
    As stated earlier, accelerometer may be designed in the open-loop mode to avoid the cost of electronics. This presents some challenges of its own. Open loop operation requires designing for an entirely different set of constraints in which the motion of the proof mass is also important. That may present a problem while integrating this with the current design.

4. REFERENCES

1. ADXL50 Data Sheet by Analog Devices.
2. Siedel H., Csepregi L., "*Design Optimization for Cantilever-type Accelerometers*", Sensors and Actuators, 6 (1984) 81-92.
3. Engesser M., Franke A.R., Maute M., Meisel D.C., Krovink, J.G., "*A robust and flexible optimization technique for efficient shrinking of MEMS accelerometers*", Microsystems Technology (2010), 16: 647-654.
4.*MEMS Accelerometers*, Seminar, University of Ljubljana, Faculty for mathematics and physics, Department of physics, Andrejašic M. March 2008.
5. Leu G.,Simion S., Serbanescu A., *"Mems Optimization Using Genetic Algorithms",* IEEE 2004.
6. Coultate J.K., Fox C.H.J, McWilliam S., Malvern A.R., *"Application of optimal and robust design methods to a MEMS accelerometer",* Sensors and Actuators A 142 (2008) 88–96.
7.Liu Y., Yang H., Wang G., "*Genetic Algorithm Based Multidisciplinary Design Optimization of MEMS Accelerometer*", Applied Mechanics and Materials Vols. 101-102 (2012) pp 530-533.
8. Lawrence A., *Modern Inertial Technology*, second edition, Springer, NewYork, 1998.

APPENDIX: MATLAB CODE USED FOR OPTIMIZATION

MATLAB Code Used in Optmization:

```
      % main  function
clear all


% include frequency constraint and etching constraint
global rho eta h E e0 tol_for_amin tol_for_FSR
rho = 2330;     %density of silicon
eta = 1.66e-5;  %Viscosity of N2
h   = 135e-6;   %height of wafer
e0  = 8.85e-12; %perimitivity of free space
E   = 1.3e11;   %Young's modulus of silicon<100>
% tol_for_amin = 1.937e-4; %Constraint tuning
 %tol_for_FSR = -6.35e2;

%      1      2     3        4       5    6       7    8   9
%[    l_s,    w_s,  w_p,     l_p,    N,  l_f,    w_f,  V0, t]



%x0 = [1000e-6  15e-6 500e-6  400e-6  10  200e-6  20e-6 5  2e-6]';

x0=[0.00126393510406163;1.01574251303284e-
05;0.00149999997976023;0.00460662436296896;10.0000000000202;0.001258150134063
35;2.99999797602247e-05;4.99999650803381;2.79679198427834e-06]';


lb = [100e-6  2e-6  200e-6   5e-6    10  100e-6  3e-6  0.1  1e-6]';
ub = [4000e-6 75e-6 1500e-6 5000e-6 600 4000e-6 30e-6  5    3e-6]';

Aineq=[-1     0     0        0       0   1       0     0  0;    ...
        2     0     1        0       0   0       0     0  0;    ...
        0     2     0        1       0   0       0     0  0];
bineq=[0;5e-3;5e-3];

  options =
optimoptions('fmincon','MaxFunEvals',2000000,'MaxIter',100000,'Algorithm','sq
p','Display','iter');
 [xopt1,fval,exitflag,output,lambda,grad,hessian]=fmincon(@a_min, x0, Aineq,
bineq,[],[], lb,ub, @nonlcon,options);


 opts=optimset('Algorithm','sqp','TolCon',1e-15,'useParallel','always');
 problem=createOptimProblem('fmincon','objective',@FSR,
'Aineq',Aineq,'bineq',bineq,'x0',x0,'lb',lb,'ub',ub,'nonlcon',@nonlcon,'optio
ns',opts);
 ms= MultiStart;
 %[xopt fval]= fmincon(problem)
 [xopt, fval, eflag, output, manymins]=run(ms,problem,500);
 fval
```

%%%

```
function [c,ceq]=nonlcon(x)



    l_s=x(1);
    w_s=x(2);
    w_p=x(3);
    l_p=x(4);
    N=x(5);
    l_f=x(6);
    w_f=x(7);
    V0=x(8);
    t=x(9);

    c(1)=Critical_Voltage(N,l_f,t,l_p,w_p,w_f,w_s,l_s,V0);
    c(2)=damping_const(l_f,w_p,w_f,N,w_s,l_s,t,l_p); % Done
    c(3)=stiff_ratio_inout(l_p,w_p,w_f,l_f,N,w_s,l_s);%Done
    c(4)=stiff_ratio_intrans(l_p,w_p,w_f,l_f,N,w_s,l_s);%Done
    c(5)=geom_const1(N,t,w_f,l_p); %Done
    c(6)=first_mode(l_p,w_p,w_f,l_f,N,w_s,l_s);
    c(7)=mode_separation(l_p,w_p,w_f,l_f,N,w_s,l_s);
   %c(8)=a_min_as_constraint(l_p,w_p,w_f,l_f,N,w_s,l_s,t);
   %c(9)=FSR_as_constraint(N,l_f,V0,t,l_p,w_p,w_f) ;

    ceq=[];


%%%%%%%%%%%%%%%%%%%%%%%%%%%%%%%%%%%%%%%%%%%%%%%%%%%%%%%%%%%%%%%%%%%%%%%%%%%%

%a_min
function a=a_min(x)
    global rho eta h E e0
    l_s=x(1);
    w_s=x(2);
    w_p=x(3);
    l_p=x(4);
    N=x(5);
    l_f=x(6);
    w_f=x(7);
    V0=x(8);
    t=x(9);

    A=l_f*h;         %Area
    C0=e0*A/t;        %intial Capacitance


    delC_min=4e-18; %minimimum measurable capacitance
    m=mass(l_p,w_p,w_f,l_f,N);
    k=m*((2*pi)*nat_freq_in_plane(l_p,w_p,w_f,l_f,N,w_s,l_s) )^2 ;
%In plane stiffness

    a=k*t*delC_min/(m*C0);
%%%%%%%%%%%%%%%%%%%%%%%%%%%%%%%%%%%%%%%%%%%%%%%%%%%%%%%%%%%%%%%%%%%%%%%%%%%%
```

```
function amax=FSR(x)

    l_s=x(1);
    w_s=x(2);
    w_p=x(3);
    l_p=x(4);
    N=x(5);
    l_f=x(6);
    w_f=x(7);
    V0=x(8);
    t=x(9);


    global rho eta h E e0

    amax= -N*e0*h*l_f*V0^2*((0.8/t^2))/(mass(l_p,w_p,w_f,l_f,N));
end

%%%%%%%%%%%%%%%%%%%%%%%%%%%%%%%%%%%%%%%%%%%%%%%%%%%%%%%%%%%%%%%%%%%%%%%%%%%%

function a=a_min_as_constraint(l_p,w_p,w_f,l_f,N,w_s,l_s,t)
    global rho eta h E e0 tol_for_amin


    A=l_f*h;         %Area
    C0=e0*A/t;        %intial Capacitance


    delC_min=4e-18; %minimimum measurable capacitance
    m=mass(l_p,w_p,w_f,l_f,N);
    k=m*((2*pi)*nat_freq_in_plane(l_p,w_p,w_f,l_f,N,w_s,l_s) )^2 ;
%In plane stiffness

    a=k*t*delC_min/(m*C0)-tol_for_amin;
%%%%%%%%%%%%%%%%%%%%%%%%%%%%%%%%%%%%%%%%%%%%%%%%%%%%%%%%%%%%%%%%%%%%%%%%%%%%
function amax=FSR_as_constraint(N,l_f,V0,t,l_p,w_p,w_f)

global rho eta h E e0 tol_for_FSR

    amax= -N*e0*h*l_f*V0^2*((0.8/t^2))/(mass(l_p,w_p,w_f,l_f,N))-tol_for_FSR;

%%%%%%%%%%%%%%%%%%%%%%%%%%%%%%%%%%%%%%%%%%%%%%%%%%%%%%%%%%%%%%%%%%%%%%%%%%%%
function C=Critical_Voltage(N,l_f,t,l_p,w_p,w_f,w_s,l_s,V0)
    global rho eta h E e0
    %delfdelx=N*e0*h*l_f*V0^2/(2*t^3);
    m=mass(l_p,w_p,w_f,l_f,N);
    k=m*(2*pi*nat_freq_in_plane(l_p,w_p,w_f,l_f,N,w_s,l_s))^2;
    Vcrit=sqrt(k*t^3/(2*e0*l_f*h*N));
    %eps=1;
    C=V0-Vcrit;


%%%%%%%%%%%%%%%%%%%%%%%%%%%%%%%%%%%%%%%%%%%%%%%%%%%%%%%%%%%%%%%%%%%%%%%%%%%%
```

```
function C = damping_const(l_f,w_p,w_f,N,w_s,l_s,t,l_p)
    global rho eta h E e0
    b=96*eta*l_f*h^3*N/(pi^4*t^3); %damping constant
    m=mass(l_p,w_p,w_f,l_f,N);
    k=m*(2*pi*nat_freq_in_plane(l_p,w_p,w_f,l_f,N,w_s,l_s))^2;
    gamma=b/(2*sqrt(k*m));            %damping ratio
    eps=0.1;
    C=abs(gamma-0.707)-eps;


%%%%%%%%%%%%%%%%%%%%%%%%%%%%%%%%%%%%%%%%%%%%%%%%%%%%%%%%%%%%%%%%%%%%%%%%%%%%

function m=first_mode(l_p,w_p,w_f,l_f,N,w_s,l_s)

    m=1e3-nat_freq_in_plane(l_p,w_p,w_f,l_f,N,w_s,l_s);


%%%%%%%%%%%%%%%%%%%%%%%%%%%%%%%%%%%%%%%%%%%%%%%%%%%%%%%%%%%%%%%%%%%%%%%%%%%%

function g=geom_const1(N,t,w_f,l_p)
%fingers should fit on proof mass
g=N*(2*t+w_f+1e-6)-l_p;

%%%%%%%%%%%%%%%%%%%%%%%%%%%%%%%%%%%%%%%%%%%%%%%%%%%%%%%%%%%%%%%%%%%%%%%%%%%%

 function m=mass(l_p,w_p,w_f,l_f,N)
global rho eta h E e0
m=rho*h*l_p*w_p+N*rho*h*l_f*w_f;
end


%%%%%%%%%%%%%%%%%%%%%%%%%%%%%%%%%%%%%%%%%%%%%%%%%%%%%%%%%%%%%%%%%%%%%%%%%%%%

function k=mode_separation(l_p,w_p,w_f,l_f,N,w_s,l_s)
    diff=1e4;
    k=diff-
nat_freq_out_plane(l_p,w_p,w_f,l_f,N,w_s,l_s)+nat_freq_in_plane(l_p,w_p,w_f,l
_f,N,w_s,l_s);


%%%%%%%%%%%%%%%%%%%%%%%%%%%%%%%%%%%%%%%%%%%%%%%%%%%%%%%%%%%%%%%%%%%%%%%%%%%%

function w1=nat_freq_in_plane(l_p,w_p,w_f,l_f,N,w_s,l_s)
    global rho eta h E e0
    Iy=1/12*h*w_s^3;
    m=mass(l_p,w_p,w_f,l_f,N);
    w1=1/(2*pi)*sqrt(3*N*E*Iy/(13/140*rho*w_s*h*N*l_s^4+1/4*m*l_s^3));
%%%%%%%%%%%%%%%%%%%%%%%%%%%%%%%%%%%%%%%%%%%%%%%%%%%%%%%%%%%%%%%%%%%%%%%%%%%%

function w2=nat_freq_out_plane(l_p,w_p,w_f,l_f,N,w_s,l_s)
    global rho eta h E e0
    %m=mass(l_p,w_p,w_f,l_f,N);
    L=l_s;
    e=l_p;
    I1=N/2*(1/12*w_s*h^3);
    I2=1/12*w_p*h^3;
```

```
    Int1=L^3/(12*(E*I1));            % Different integrals
    Int2=1/(E*I2)*((L+e/2)^3-L^3)/3;
    Int4=rho*h*N*w_s/(2*E*I1)*(0.0026*L^7);
    m_f= N*rho*h*l_f*w_f;            % Mass of fingers
    constant=m_f/e+rho*w_p*h/(E*I2)^2;
    part1=((L+e/2)^7-L^7)/(7*36);
    part2=1/3*(L+e/2)^4*(e/4)^3;
    part3=L^6/36*(0.5*I2/I1+1)^2*e/2;
    part4=-1/6*(L+e/2)^2*(((L+e/2)^5-L^5)/5-L/4*((L+e/2)^4-L^4));
    part5=2*L^3/36*(1/2*I2/I1+1)*((L+e/2)^4-L^4)/4;
    part6=L^3/6*(1/2*I2/I1+1)*(L+e/2)^2*((L+e/2)^2/4-L^2/4-L*e/4);
    Int5=constant*(part1+part2+part3+part4+part5+part6);
    w2=sqrt((Int1+Int2)/(Int4+Int5));

%%%%%%%%%%%%%%%%%%%%%%%%%%%%%%%%%%%%%%%%%%%%%%%%%%%%%%%%%%%%%%%%%%%%%%%%%%%%

function C=stiff_ratio_inout(l_p,w_p,w_f,l_f,N,w_s,l_s)

global rho eta h E e0
Iz=h^3*w_s/12;
Kz=12*E*Iz/l_s^3;
Kx=mass(l_p,w_p,w_f,l_f,N)*(2*pi*nat_freq_in_plane(l_p,w_p,w_f,l_f,N,w_s,l_s)
)^2;

C=10-Kz/Kx;

%%%%%%%%%%%%%%%%%%%%%%%%%%%%%%%%%%%%%%%%%%%%%%%%%%%%%%%%%%%%%%%%%%%%%%%%%%%%

function C=stiff_ratio_intrans(l_p,w_p,w_f,l_f,N,w_s,l_s)

global rho eta h E e0
Iy=h*w_s^3/12;
Ky=E*w_s*h/l_s;
Kx=mass(l_p,w_p,w_f,l_f,N)*(2*pi*nat_freq_in_plane(l_p,w_p,w_f,l_f,N,w_s,l_s)
)^2;


C=5-Ky/Kx;
%%%%%%%%%%%%%%%%%%%%%%%%%%%%%%%%%%%%%%%%%%%%%%%%%%%%%%%%%%%%%%%%%%%%%%%%%%%%
```